Discovery of New Vega-type Systems From IRAS and the 2-Micron All-Sky Survey (2MASS)

Sergio B. Fajardo-Acosta

Jet Propulsion Laboratory, California Institute of Technology,

Infrared Processing and Analysis Center, MS 100-22, Pasadena, CA 91125;

fajardo@ipac.caltech.edu

Charles A. Beichman

Jet Propulsion Laboratory, MS 180-703, 4800 Oak Grove Drive, Pasadena, CA 91109;

chas@pop.jpl.nasa.gov

Roc M. Cutri

California Institute of Technology, Infrared Processing and Analysis Center, MS 100-22,

Pasadena, CA 91125; roc@ipac.caltech.edu

Received ______________________; accepted ______________________

ABSTRACT

We obtained J (1.25 μm), H (1.65 μm), and K_s (2.17 μm) photometry from the 2-Micron All-Sky Survey (2MASS), and 12, 25, 60, and 100 μm photometry from the IRAS Faint Source Catalog (FSC), of a sample of 2928 field stars. We selected 308 main-sequence (luminosity class IV, IV–V, or V) stars from this sample. The main-sequence luminosity classes in these systems were either previously known (165 stars), or determined from their Hipparcos distances and spectral types or JK_s colors (107 stars), or modeled from their JHK_s colors (36 stars). We searched for main-sequence stars in this sample with 12 μm excess emission, with respect to the expectation of photospheric emission at J, H, and K_s. We discovered 10 systems with 12 μm excess emission, newly reported here. The excess emission in these systems is likely to be from Vega-type circumstellar dust. Simple models of the excess emission show that dust in these systems is at "terrestrial material" temperatures of $\sim$ 200–500 K, located at $\sim$ 1 AU from the stars. Plaussibly colder dust in the systems, located further out from the stars, could not be measured with IRAS. The exception is HD 93331 (B9.5 V), previously known for its IRAS far-infrared excess, and newly reported here for its 12 μm excess. This system is likely to be spatially resolved with current imaging technology.

Subject headings: circumstellar matter—dust, extinction—infrared: stars

1. Introduction

The detection of main-sequence circumstellar dust systems provides a powerful tool in the study of possible planetary systems similar to our own. The possibilities of detection of young, terrestrial-type planets similar to our own, can be directly investigated if we detect ambient circumstellar dust at terrestrial material temperatures, with which these planets can interact (Backman 1998). The first detected main-sequence system with terrestrial temperature or "exozodiacal" material around it was β Pictoris (Aumann et al. 1984; Smith & Terrile 1984). Since then, there have been more recent additional detections of exozodiacal circumstellar dust: ζ Lep, A2 Vann (Aumann & Probst 1991; Fajardo-Acosta, Telesco, & Knacke 1998); HD 98800, K5 V (Skinner, Barlow, & Justannont 1992; Zuckerman & Becklin 1993); SAO 26804, F8 V (Skinner et al. 1995); SAO 206462, F8 V (Coulson & Walther 1995), HD 100546, B9 V (Waelkens et al. 1996), HR 2174A, A3 V, and β UMa, A1 V (Fajardo-Acosta, Telesco, & Knacke 1998), and HR 4796A, A0 V (Koerner et al. 1998), among others. The warm dust in these systems is located at distances $\sim$ 10 AU from the stars. We want to know how dust at these locations is correlated with the existence of planets.

We also want to investigate this correlation with cooler circumstellar dust, located beyond the plausible planetary regions of these systems, analogously to the Kuiper Belt of our solar system. The latter regions are typically located $\sim$ 50–100 AU from the stars, and their spectral energy distributions (SEDs) peak at $\sim$ 25–60 μm (Backman & Paresce 1993). The fraction of main-sequence stars with cool circumstellar dust (Kuiper Belt-type) is an order of magnitude larger than the fraction with warm, exozodiacal-type dust ((Aumann & Probst 1991). Eventually we want to know the frequency of occurrence of main-sequence circumstellar dust, currently known only approximately from IRAS and ISO surveys; at least $\sim$ 15 % of main-sequence stars are believed to have dust (Backman & Paresce

1993; Plets 1997; Dominik & HJHVEGA Consortium 1998; Mannings & Barlow 1998; Fajardo-Acosta et al. 1999).

Towards the ellucidation of the frequency of occurrence of main-sequence circumstellar dust, particularly of exozodiacal type, we present the results of a survey employing a novel technique: we used the 2-Micron All-Sky Survey (2MASS, Skrutskie et al. 1997) to obtain near-infrared SEDs of stars, and IRAS 12 μm photometry to thus search for 12 μm excesses, presumably from exozodiacal dust.

2. Observational Data From 2MASS and IRAS

We extracted 12, 25, 60, and 100 μm photometry of sources from the IRAS Faint Source Catalog, version 2 (Moshir et al. 1992, hereafter FSC). We required that the sources be located more than 20° away from the galactic plane, that their 12 μm photometry be of moderate to high quality, and that they have at most one 100 μm-only neighboring source (to minimize confusion with cirrus). We then extracted J (1.25 μm), H (1.65 μm), and K_s (2.17 μm) photometry from 2MASS point sources located within the IRAS positional error ellipse of any of the FSC sources extracted above. The 2MASS sources were required to have J, H, and K_s magnitudes > 5, or else their photometry saturates even in the shortest 2MASS exposures of 51 ms [1] The 2MASS sources were also required to be located within 6 arcsec of a stellar source in the ACT Reference Catalog (Urban, Corbin, & Wycoff 1997), or the USNO-A.2 Catalog (Monet et al. 1998). Typically, our selected 2MASS sources were actually < 1 arcsec from a star in the above catalogs. We further required that our 2MASS

---

[1]See the Explanatory Supplement to the 2MASS Second Incremental Data Release by R. M. Cutri et al., which is at http://www.ipac.caltech.edu/2mass/releases/second/doc/explsup.html.

point sources were not located within 5 arcsec of the peak of a 2MASS extended source. We removed purious multiple 2MASS point sources associated to moderately bright stars, and other sources affected by 2MASS artifacts (meteor trails, diffraction spikes, scattered light, latent images, and "stripes" due to nearby bright stars, as described in the Explanatory Supplement to the 2MASS Second Incremental Data Release.

The above 2MASS, IRAS FSC, and ACT/USNO-A.2 optical star associations yielded 2928 sources. In these associations there was a unique 2MASS source inside the IRAS error ellipse of an FSC one. There were 1975 stars from the ACT Catalog, and 953 from the USNO-A.2 Catalog. We obtained an additional 1708 known giant and supergiant stars, but we do not consider them further here.

3. Selection of Main-Sequence Stars

Our goal is to select stars of luminosity classes IV, IV-V, or V, collectively referred to here as "main-sequence" stars, from the above 2MASS-IRAS-optical star associations. To this end we obtained SIMBAD spectral types and luminosity classes and determined that 165 stars in our sample are on the main-sequence. For the rest of our sources, we attempted to determine their luminosity classes, either from their position in a color-magnitude diagram, or from their JHK_s colors, as explained below.

We obtained Hipparcos Catalog (Perryman et al. 1997) distances and SIMBAD, ACT or Hipparcos Catalog V (visual) magnitudes of 507 stars. We plotted a color-magnitude diagram (absolute visual magnitude M_V vs. $J - K_s$ color, Figure 1), in order to estimate the luminosity class of the above sources. We have not included the effects of interstellar extinction on M_V, but we do not think they are significant because of our selection constraint on galactic latitude (Section 2). The color $J - K_s$ is a good discriminator of spectral type (Koornneef 1983; Bessell & Brett 1988). Figure 1 shows that most of our stars with $J - K_s \gtrsim 0.48$ (later than $\sim$ G5) are giants and supergiants, whereas practically all stars in our sample earlier than G5 are on the main-sequence. From Figure 1, we determined that 107 of the 507 sources plotted are on the main-sequence.

There are 2261 stars in our sample without Hipparcos distances and without SIMBAD luminosity classes, but with complete JHK_s 2MASS photometry. We attempted to estimate their luminosity classes (and spectral type when previously unknown) by means of $J - K_s$, $H - K_s$ models by Koornneef (1983) or Bessell & Brett (1988). In Figure 2 we plot the color-color diagram of these stars, together with Koornneef models for main-sequence (class V), giant (class III), and supergiant (class I) stars. These three models are indistinguishable for stars with $J - K_s \lesssim 0.83$ (earlier than M0). We estimate that 36 stars in this sample are late-type main-sequence stars, but 7 of these stars are actually beyond the Koornneef model. The latter 7 stars might be dwarfs of spectral type later than $\sim$ M8.

From the above three methods (SIMBAD, color-magnitude diagram, or color-color diagram) we determined that 308 stars in our sample are approximately of main-sequence class.

4. Identification of 12 μm Excesses

In this section we identify the main-sequence stars (out of the 308 above ones) that show 12 μm excess emission, with respect to the extrapolation of photospheric flux estimated from 2MASS JHK_s photometry.

We computed $K_s-[12]$ colors of the 308 stars, where the IRAS 12 μm magnitude ([12], Beichman et al. 1988) was formed after applying a color-correction, assuming a 10^4 K blackbody SED. The color-correction will differ for other blackbody temperatures, but only up to ~ 5 % in the range 2000–10000 K from the 10^4 K result (Beichman et al.). We have included uncertainties of ~ 4 % (from absolute calibration) and ~ 5 % (from color-correction) (Beichman et al.) in the 12 μm IRAS magnitudes. Figure 3a shows the K_s−[12] vs. $J - K_s$ color-color diagram of the 308 stars from Section 3. Normal main-sequence stars (without 12 μm excesses) have K_s−[12] ~ 0 mag. in Figure 3a. Sources with 12 μm excesses, located above the majority of normal stars in Figure 3a, have K_s−[12] ~ 0.5.

In order to more precisely define a 12 μm excess, we first obtained the mean K_s−[12] ($\overline{K_s - [12]_{bin}}$) and standard deviation σ_{bin} (plotted in Figure 3b as a thick line connecting points with thick error bars) in bins of $J - K_s$ about 0.15 mag. wide, which roughly span one whole spectral type. We iteratively excluded stars from the computation of $\overline{K_s - [12]_{bin}}$ if initially $Ks - [12] - \sigma > \overline{K_s - [12]_{bin}} + \sigma_{bin}$, where σ is the measurement error of each star (Figure 3a). There were 10 stars that satisfied this criterion, and we henceforth refer to them as having 12 μm excess emission. These stars are plotted in Figures 3a and 3b, as filled squares. Of these, 5 are also plotted in Figure 1. We did not find stars, whose main-sequence class we determined with JHK_s colors (Figure 2), with reliable 12 μm excess emission, as discussed at the end of this section.

In Table 1 we list the 10 main-sequence stars with 12 μm excesses, the method or source for estimating their main-sequence luminosity class, and their $J - K_s$, K_s−[12] colors, as well as other characterstics of the stars. We quantify the excess emission of a star by Excess $K_s - [12] = K_s - [12] - \overline{K_s - [12]_{bin}}$ and its uncertainty by $(\sigma^2 + \sigma_{bin}^2/n_{bin})^{1/2}$, where n_{bin} is the number of stars in each bin of $J - K_s$ (ranging from 16 $\sim$ B stars to 91 $\sim$ F stars). Table 2, column [2] lists Excess $K_s - [12]$ for the 10 stars with excesses. It also lists (in column [3]) this excesses relative to bin and measurement errors: Rel. Excess $K_s - [12] = (\text{Excess}K_s - [12])/(\sigma^2 + \sigma_{bin}^2)^{1/2}$. Table 2 shows that most of our sources had relative excesses $\gtrsim 2\sigma$.

We had originally found 7 more stars with apparent weak excesses (not shown in Figures 3a or 3b and not listed in Tables 1 or 2). Their relative excesses were $< 2\sigma$. Among these sources, 4 stars later than G7 type (TYC 2246 00788 1, M0–M1, HD 15119, G8 IV, HD 31904, G8 IV, and SAO 149225, K5) had photospheric SEDs (such as those computed in Section 5) more consistent with giant rather than main-sequence stars. Namely, their JHK_s flux densities indicated photospheric temperatures $\lesssim$ 4500 K, lower by 500–1000 K than for main-sequence stars of their respective spectral type (Allen 1973; Gray & Corbally 1994). These cooler photospheric SEDs encompassed their IRAS 12 μm flux densities, within their errors. We also found 2 stars (HIP 84102, G5–G9, and USNO-A.2 105020799879, K8–M7) with very large K_s–[12] ($\sim$ 2.0), and with V mag. > 10. We doubt the infrared 12 μm source is really associated with such faint optical counterparts. The infrared source is perhaps an embedded object such as a late-type giant/supergiant star with a dust shell, in each of these cases. Our original estimate of main-sequence class for TYC 2246 00788 1, SAO 149225, and USNO-A.2 105020799879 was based on their JHK_s 2MASS colors (Figure 2).

We found one eclipsing binary of W Ursa Majoris type, with a 12 μm excess: BV Dra (F7 V), part of the BV/BW Dra contact binary system (16 arcsec separation, McGale, Pye, & Hodgkin 1996, among others). This system is an X-ray emission source (J1511.8+6151) in the ROSAT Catalog (White, Giommi, & Angelini 1995), whose emission can be modeled from optically thin plasma (McGale et al.). The 12 μm excess emission must also arise from this plasma. We did not consider this system further here.

A source of possible spurious 12 μm excess emission is neighboring patches of warm ISM emission around our stars. We checked the IRAS Sky Survey Atlas (ISSA) images around our stars, via the IRSKY and ISSA Visualizer services at IPAC, to look for excessive cirrus and warm ISM sources close to them. We found that the ambient ISSA regions of the sources were mostly clean around the stars, primarily because of their high galactic latitudes. The only exception is HD 150697, located at the edge of the ρ Oph star-forming region. We saw an abundance of contaminating cirrus and 12 μm emission sources close to the star (within $\sim$ few arcmin). Therefore the excess of this star needs to be treated with caution.

The 12 μm excesses in our sources (Table 1) cannot be an artifact arising from "flux overestimation" in the IRAS FSC (Moshir et al. 1992). This overestimation occurs in a sample of sources with measurement errors, where the number of sources decreases with increasing source brightness. More sources are "moved up" in flux density than "moved down," because of their errors. In addition, if sources are chosen to satisfy a threshold S/N, then faint sources close to the threshold might be statistically "moved out" of the distribution. By this effect, faint 12 μm sources with S/N $\sim$ 6 in the IRAS FSC might have flux densities overestimated by $\sim$ 12 % (from Moshir et al.). In our sample of excess stars, their 12 μm flux densities have S/N $\sim$ 6 (Table 1, column [9]), and these flux densities are $\sim$ 66 % above those expected in normal stars (Table 2, column [2]). The 12 μm excesses are therefore much higher than the effects of flux overestimation.

5. SEDs of Newly Identified Main Sequence Stars With 12 μm Excesses

The absolute calibration of 2MASS photometry is presently unknown, but we approximately calibrated it with the zero-magnitude JHK flux densities by Tokunaga (1986). Together with the absolute calibration and color-correction of IRAS photometry (Beichman et al. 1988) we constructed the 2MASS-IRAS FSC SEDs of the stars in Table 1. In this way we can begin to infer physical characteristics of plausible circumstellar systems.

The IRAS FSC flux densities of all stars in Table 1, except HD 93331, are only 3 σ upper limits at 25–100 μm. The 12 μm flux densities are of moderate quality for HD 93331, and of high quality for all the other sources. We used the IRAS ADDSCAN/SCANPI scan-coadding program at IPAC, and we verified that all the stars in Table 1 are point sources at 12 μm. We also obtained a weak detection of a point source at 60 μm for HD 97854 (footnote to Table 1). The IRAS flux densities of HD 93331 are all of moderate-to-high quality, and had allowed a detection of a far-infrared excess (at 25–100 μm) in this object (Mannings & Barlow 1998). The 12 μm excess in HD 93331 is newly reported here.

In Figure 4 we show the 2MASS-IRAS FSC SED of HD 93331. The photospheric SED (solid line in Figure 4) is a Kurucz (1992) model with solar metallicity, $\log(g) = 4.0$ (g is surface gravity), and $T_{eff} = 10,000$ K, closely approximating the 10,300 K T_{eff} for a B9.5 V star (Gray & Corbally 1994). The Kurucz fit is identical in the 2MASS and IRAS wavelengths to that from a hot blackbody (of temperature $\gtrsim$ 12,000 K) for this and other early-type stars. The IRAS excess above the photospheric SED is clearly evident in Figure 4. We could not fit all the IRAS excess fluxes with a single-temperature blackbody. But we could fit the 12 and 25 μm excess fluxes with a warm (238 K) blackbody SED, and the 25 and 60 μm fluxes with a colder blackbody, at 86 K. These characteristic blackbody temperatures are determined well to within $\sim$ 10 %. The SED of HD 93331 is clearly inconsistent with free-free emission (which would make the excess flux density decrease with increasing wavelength).

Since only one IRAS excess flux is reliably known for most of the other sources in Table 1, there is no assurance that their excess emission is from circumstellar dust. But there is no observational evidence of stellar activity in these main-sequence stars that would hint at plasma emission being significant. The unusual case of BV Dra was discussed in Section 4.

The sources in Tables 1 and 2 are not in the ROSAT Catalog (White, Giommi, & Angelini 1995), and there are no indications of variability in the literature. Therefore, we explore the possibility that their excess emission is from circumstellar dust.

Table 2 lists the blackbody temperature (T_{dust}, column [4]) of simple dust models fit to the 12 and 25 μm flux densities of our 10 stars. Except for HD 93331 above, the fits at wavelengths $\geq 25\mu$m to upper limit fluxes are only speculative. But the fit at 12–25 μm can yield a lower limit to the temperature of a possible warm dust component. These lower-limit T_{dust} values were $\sim$ 210–500 K around our stars. It is also possible that there exists a colder dust component further out from the stars, such as in the HD 93331 system (Figure 4). Other Vega-type systems also seem to have a warm dust region close to the star (in areas roughly the size of our solar system's planetary region), and a colder dust region further out (resembling our solar system's Kuiper Belt). The disk of β Pictoris, the prototype of Vega-type stars with warm dust at $\sim$ 280 K (Telesco & Knacke 1991; Knacke et al. 1993), also has another component of colder dust, extending outwards of 80 AU from the star, with maximum grain temperatures of $\sim$ 140 K (Backman, Gillett, & Witteborn 1992). For the rest of our sources, studies of their colder dust component will be made possible with SIRTF photometry longwards of 12 μm. It is possible that these more extended regions could also be spatially resolved with SIRTF.

The models described in Table 2 can also give us an indication of the spatial resolvability of the possible warm dust component of these systems. The quantity r_{dust} (column [5]) is the radiative equilibrium distance of blackbody grains at temperature T_{dust} from the stars. It is in this case a rough upper limit to the size of a hypothetical warm dust circumstellar component. Together with the distances D (Table 1, column [6]), r_{dust} yields the angular extent θ_{dust} of the warm regions (Table 2, column [6]). Typically θ_{dust} is $\sim$ 10 milliarcsec (mas), but notable exceptions are HD 93331 (74 mas), HIP 21377 (50 mas), HD 20980 (55 mas), and HD 150697 (28 mas). We note that HD 93331 has a colder component, whose characteristic θ_{dust} is 560 mas (see footnote to Table 2). These 4 systems are the most likely to be spatially resolved. But the disk recently imaged around HR 4796A (A0 V) is $\approx$ 70 AU or $\approx$ 1 arcsec in radius at 10 and 20 μm (Jayawardhana et al. 1998; Koerner et al. 1998; Telesco et al. 2000). Therefore, the imaging detection of the warm dust components of our sources is a formidable challenge.

Excess circumstellar emission can be quantified and compared to other systems by means of the fractional dust luminosity τ. It is defined by the ratio of integrated excess emission from dust, to integrated emission from the photosphere alone. Details of these simple computations can be seen in Fajardo-Acosta et al. 1999). The excess emission was integrated from 1 μm (where it is practically zero) to 12 μm (where it is unambiguously detected). The integral of excess emission has its highest contributions at higher frequencies than in the far-infrared. In this sense, values of τ so obtained are lower limits for all sources except HD 93331. For the latter we integrated the warm (238 K) component from 1 to 25 μm, and the colder (86 K) component from 25 μm to 100 μm. The latter yielded a 2 % contribution to the integral of excess flux.

Values of τ (Table 2, column [7]) ranged from 6×10^{-5} (HD 97854) to 2×10^{-3} (HD 93331). For comparison, previuosly known systems with $\tau \sim 10^{-3}$ are β Pic, HR 4796A, 49 Cet, 51 Oph, and HD 98800 (Jura et al. 1993; Zuckerman & Becklin 1993). High values of τ can result from the presence of warm dust, such as in systems with 12 μm excesses, as opposed to colder dust with excesses longwards of 25 μm in systems such as Vega itself.

The presence of significant 12 μm excess emission in our selected stars implies they are excellent targets for mid-infrared intermediate-resolution spectroscopy. In this way we can search for silicate dust analogous to that in β Pic's disk and solar system comets (Knacke et al. 1993). The system HD 93331 could conceavably be spatially resolved at 10 and/or

20 μm with the Keck or Gemini telescopes, since the angular extent of its cold component (Table 2) is 0.56 arcsec, although this observation will be challenging.

We thank the 2MASS staff at IPAC, Harold Corwin, and Laurent Cambresy for insightful discussions. S. F.-A. and C. B. acknowledge the support of the Jet Propulsion Laboratory, California Institute of Technology, which is operated under contract with the National Aeronautics and Space Administration. The research has made use of the SIMBAD database, operated at CDS, Strasbourg, France. This publication makes use of data products from the 2-Micron All Sky Survey, which is a joint project of the University of Massachusetts and the Infrared Processing and Analysis Center/California Institute of Technology, funded by the National Aeronautics and Space Administration and the National Science Foundation.

REFERENCES

Allen, C. W. 1973, Astrophysical Quantities (London: Athlone Press)

Aumann, H. H., Gillett, F. C., Beichman, C. A., de Jong, T., Houck, J. R., Low, F. J., Neugebauer, G., Walker, R. G., & Wesselius, P. R. 1984, ApJ, 278, L23

Aumann, H. H., & Probst, R. G. 1991, ApJ, 368, 264

Backman, D. E., Gillett, F. C., & Witteborn, F. C. 1992, ApJ, 385, 680

Backman, D. E., & Paresce, F. 1993, in Protostars and Planets III, ed. E. H. Levy, J. I. Lunine, & M. S. Mathews (Tucson: Univ. Arizona Press), 1253 (BP93)

Backman, D. E. 1998, in Exozodiacal Dust Workshop, NASA CP 1998-10155, ed. D. E. Backman, L. J. Caroff, S. A. Sandford, & D. H. Wooden (Moffett Field: NASA Ames), 107

Beichman, C. A., Neugebauer, G., Habing, H. J., Clegg, P. E., & Chester, T. J. 1988, IRAS Catalogs and Atlases: Explanatory Supplement (Washington: GPO)

Bessell, M. S., & Brett, J. M. 1988, PASP, 100, 1134

Dominik, C., & HJHVEGA Consortium 1998, Ap&SS, 255, 103

Fajardo-Acosta, S. B., Telesco, C. M., & Knacke, R. F. 1998, AJ, 115, 2101

Fajardo-Acosta, S. B., Stencel, R. E., Backman, D. E., & Thakur, N. 1999, ApJ, 520, 215

Gray, R. O., & Corbally, C. J. 1994, AJ, 107, 742

Jayawardhana, R., Fisher, S., Hartmann, L., & Telesco, C. 1998, ApJ, 503, L79

Knacke, R. F., Fajardo-Acosta, S. B., Telesco, C. M., Hackwell, J. A., Lynch, D. K., & Russell, R. W. 1993, ApJ, 418, 440

Koornneef, J. 1983, A&A, 128, 84

Koerner, D. W., Ressler, M. E., Werner, M. W., & Backman, D. E. 1998, ApJ, 503, L83

Kurucz, R. L. 1992, in Stellar Population of Galaxies, IAU Symp. 149, ed. B. Barbuy & A. Renzini (Dordrecht: Kluwer), 225

Mannings, V., & Barlow, M. J. 1998, ApJ, 497, 330

McGale, P. A., Pye, J. P., & Hodgkin, S. T. 1996, MNRAS, 280, 627

Monet, D., et al. 1998, USNO-A.2 Catalog (Flagstaff: USNO)

Moshir, M. et al. 1992, Explanatory Supplement to the IRAS Faint Source Survey, Version 2, JPL D-10015 8/92 (Pasadena: JPL) (FSC)

Perryman, M. A. C., et al. 1997, A&A, 323, L49 (Hipparcos Catalog)

Plets, H. 1997, Ph.D. Thesis, Katholieke Universitet Leuven

Skinner, C. J., Barlow, M. J., & Justtanont, K. 1992, MNRAS, 255, 31P

Skinner, C. J., Sylvester, R. J., Graham, J. R., Barlow, M. J., Meixner, M., Keto, E., Arens, J. F., & Jernigan, J. G. 1995, ApJ, 444, 861

Skrutskie, M. F. 1997, The Impact of Large Scale Near-IR Sky Surveys, ed. F. Garzon et al. (Dordrecht: Kluwer), 25

Smith, B. A., & Terrile, R. J. 1984, Science, 226, 1421

Telesco, C. M., & Knacke, R. F. 1991, ApJ, 372, L29

Telesco, C. M., et al. 2000, ApJ, 530, 329

Tokunaga, A. T. 1986, NASA IRTF Photometry Manual (Honolulu: Univ. Hawaii)

Urban, S.E., Corbin, T.E., & Wycoff G.L. 1997, ACT Reference Catalog (Washington: USNO) (ACT Catalog)

Waters, L. B. F. M., Coté, J., & Aumann, H. H. 1987, A&A, 172, 225

White, N. E., Giommi, P., & Angelini, L. 1995, The WGACAT Version of the ROSAT PSPC Catalogue, Rev. 1 (Greenbelt: HEASARC/LHEA/GSFC) (ROSAT Catalog)

Zuckerman, B., & Becklin, E. E. 1993, ApJ, 406, L25

This manuscript was prepared with the AAS LaTeX macros v4.0.

Fig. 1.— Color-magnitude diagram (absolute V magnitude vs. 2MASS $J - K_s$ color) of 507 2MASS-IRAS FSC-ACT stars with Hipparcos distances and previously unknown luminosity classes. Stars on the main-sequence (107) are shown as X*symbols.* Stars on the main-sequence with 12 μm IRAS excesses (5) are shown as *filled squares* and are discussed in Section 4.

Fig. 2.— 2MASS color-color diagram ($H - K_s$ vs. $J - K_s$) of 2261 2MASS-IRAS FSC-ACT/USNO A.2 stars without Hipparcos distances and with previously unknown luminosity classes. Koornneef (1983) color-color models are overplot for main-sequence (*solid line*), giant (*dotted line*), and supergiant (*dashed line*) stars. Using these models, we inferred that 36 stars (*filled circles*) are on the main-sequence. For legibility, we have reversed the above symbols and lines to white color in areas where too many star colors fill the background in black. There are no stars with 12 μm excesses (Section 4) in the sample plotted here.

Fig. 3.— 2MASS-IRAS FSC color-color diagrams ($K_s-[12]$ vs. $J - K_s$) of main-sequence stars. Stars with 12 μm IRAS excess emission have larger $K_s-[12]$ than normal stars. *(a)* Colors of 308 main-sequence stars, where *filled squares* indicate those with 12 μm excesses. *(b)* Stars with excesses are plotted as in *(a)*. The *thick line with thick error bars* is the 1 σ-clipped mean of the main-sequence sequence stars in *(a)*; error bars are 1 standard deviation, and the stars clipped from the mean are those with excesses. The *thin solid line* is the model of $K-[12]$ colors of normal stars obtained from the $V-[12]$ model by Waters, Coté, & Aumann (1987), and the $V - K$ model by Bessell & Brett (1988). The *dashed line* is a similar model but using the $V - K$ model by Koornneef (1983).

Fig. 4.— SED of the star HD 93331 (B9.5 V). *Filled rhombii* with error bars (1 standard deviation) are flux densites from 2MASS J, H, and K_s, and IRAS FSC 12, 25, 60, and 100 μm photometry, calibrated as explained in Section 5. The *solid line* is a solar metallicity Kurucz (1992) model with $\log(g) = 4.0$ and $T_{eff} = 10000$ K to represent the photospheric SED. The *dotted line* is a warm blackbody dust model (at 238 K) to represent dust close to

the star. The *dashed line* is a cold blackbody dust model (at 86 K) to represent dust further out from the star.

TABLE 1

2MASS-IRAS FSC-Optical Main-sequence Stars With 12 μm Excesses

2MASS Name[a]	Other Name	Type	Method For Type	V	D	$J-K_s$	K_s−[12]	$F_\nu(12\mu m)$
				(mag)	(pc)	(mag)	(mag)	(Jy)
(1)	(2)	(3)	(4)	(5)	(6)	(7)	(8)	(9)
2MASSI J1046248−132735	HD 93331[b]	B9.5 V	SIMBAD	7.25	152±19	−0.055±0.022	1.02±0.24	0.149±0.033[c]
2MASSI J0435141−094410	HIP 21377	A1m V	Hipp./H.R. Diag.	6.71	119±33	0.007±0.021	0.53±0.16	0.108±0.015
2MASSI J0322162−253516	HD 20980	A1 V	SIMBAD	6.34	138±14	0.026±0.030	0.45±0.18	0.129±0.021
2MASSI J0027300−314941	HD 2381	F2 V	SIMBAD	7.74	74.2±4.9	0.243±0.012	0.86±0.29	0.126±0.034
2MASSI J0547139−242938	HD 38787[d]	F2/F3 V	SIMBAD	8.69	130	0.251±0.031	1.34±0.20	0.086±0.015
2MASSI J1643186−140205	HD 150697[e]	F3 V	SIMBAD	8.07	98±10	0.298±0.021	0.65±0.19	0.101±0.018
2MASSI J0950029+333610	HD 85030	F5 V	SIMBAD/H.R. Diag.	7.90	238±61	0.249±0.022	0.63±0.23	0.099±0.021
2MASSW J0807261+194903	HD 67150	F8 V	SIMBAD/H.R. Diag.	7.71	97±10	0.290±0.016	0.61±0.17	0.157±0.024
2MASSI J1116328+691304	HD 97854	G0 V	SIMBAD/H.R. Diag.	8.23	81.2±5.5	0.304±0.019	0.47±0.19	0.055±0.015[f]
2MASSI J0929139+684605	HD 81438	G5 V	SIMBAD/H.R. Diag.	9.05	91.1±9.6	0.604±0.027	0.61±0.17	0.105±0.016

Note.—Column(4) lists the source of, or method to determine, spectral type/luminosity class: SIMBAD database, or color-magnitude diagram, Figure 1, ("H.R. Diag."). If two methods are given for a source, the first applies to spectral type and the second to luminosity class. Column(6) gives distances D which are from the Hipparcos Catalog (Perryman et al. 1997) if an uncertainty is quoted for D; otherwise, they are spectroscopic parallax estimates from the main-sequence star's observed K_s, its spectral type, and absolute K magnitude (Allen 1973; Koornneef 1983). The IRAS FSC 12 μm flux densities used in Column (8) (to compute [12] IRAS magnitudes) and listed in Column (9) were color-corrected assuming a 10^4 K blackbody SED, unless otherwise noted.

[a]2MASS names are given as "2MASSx Jhhmmss[.]s±ddmmss", where the "x" prefix varies depending upon which catalog the object originates, in this case "I" for the Second Incremental Data Release (March 2000) and "W" for the survey's database. The suffix conforms to IAU nomenclature convention and is the sexagesimal right ascension and declination at J2000 equinox.

[b]Far-infrared IRAS excess discussed by Mannings & Barlow 1998.

[c]$F_\nu(12\mu m)$ color-corrected assuming a 300 K blackbody SED (Section 5).

[d]Binary system

[e]Located at edge of ρ Oph star-forming region; IRAS photometry could be contaminated with cold cirrus and warm ISM patches emission.

[f]Marginal detection at 12 μm. Also detected at 60 μm with ADDSCAN/SCANPI; $F_\nu(60\mu m) = 0.07\pm0.02$ Jy.

TABLE 2

12 μm EXCESSES & SINGLE-TEMPERATURE BLACKBODY MODELS

NAME (1)	Excess $K_s-[12]$ (mag) (2)	Rel. Excess $K_s-[12]$ (σ) (3)	T_{dust} (K) (4)	r_{dust} (AU) (5)	θ_{dust} (arcsec) (6)	τ (7)
HD 93331	0.92±0.24	2.9	238[a]	11.2[a]	0.074[a]	2×10^{-3}
HIP 21377	0.46±0.16	2.1	280	6.0	0.050	7×10^{-5}
HD 20980	0.38±0.18	1.6	250	7.6	0.055	1×10^{-4}
HD 2381	0.79±0.29	2.4	320	1.4	0.019	4×10^{-4}
HD 38787	1.27±0.20	5.0	286	1.8	0.014	7×10^{-4}
HD 150697	0.58±0.19	2.3	213	2.8	0.028	1×10^{-4}
HD 85030	0.56±0.23	2.0	240	2.1	0.0088	1×10^{-4}
HD 67150	0.54±0.17	2.3	260	1.4	0.014	1×10^{-4}
HD 97854	0.43±0.19	1.8	215	1.7	0.021	6×10^{-5}
HD 81438	0.51±0.17	2.1	500	0.26	0.0028	7×10^{-4}

NOTE.—Column (2) lists $K_s-[12]$ minus the mean $K_s-[12]$ color of normal stars corresponding to the star's $J-K_s$ color (Figure 3b). Column (3) is the above excess, expressed in units of the quadratically-added standard deviations of the star's color and the mean color of normal stars (Figure 3b). Column (4) is the temperature T_{dust} of single-temperature blackbody dust models fitted to the IRAS FSC excess flux density at 12 μm and the upper limit at 25 μm. Therefore T_{dust} is a lower limit to warm dust around the stars. Column (5) lists the radiative equilibrium distance r_{dust} from the star for blackbody grains at temperature T_{dust}. Column (6) is the angular radius subtended by r_{dust} at the distances D given in Table 1. The values in columns (5) and (6) are rough upper limits for warm dust, but cooler dust could be located further out from the stars (Section 5). Column (7) is lower limit to fractional dust luminosity τ, or the ratio of integrated excess emission from dust to integrated photospheric emission.

[a]This source was detected in 25, 60, and 100 μm IRAS photometry (Mannings & Barlow 1998), unlike the rest of our sources. The warm dust model results for this star are not limits but instead are more exactly determined. In addition, we could also fit a colder blackbody model of dust located further from the star (Figure 4 and Section 5), at T_{dust} = 86 K, r_{dust} = 86 AU, and θ_{dust} = 0.56 arcsec.

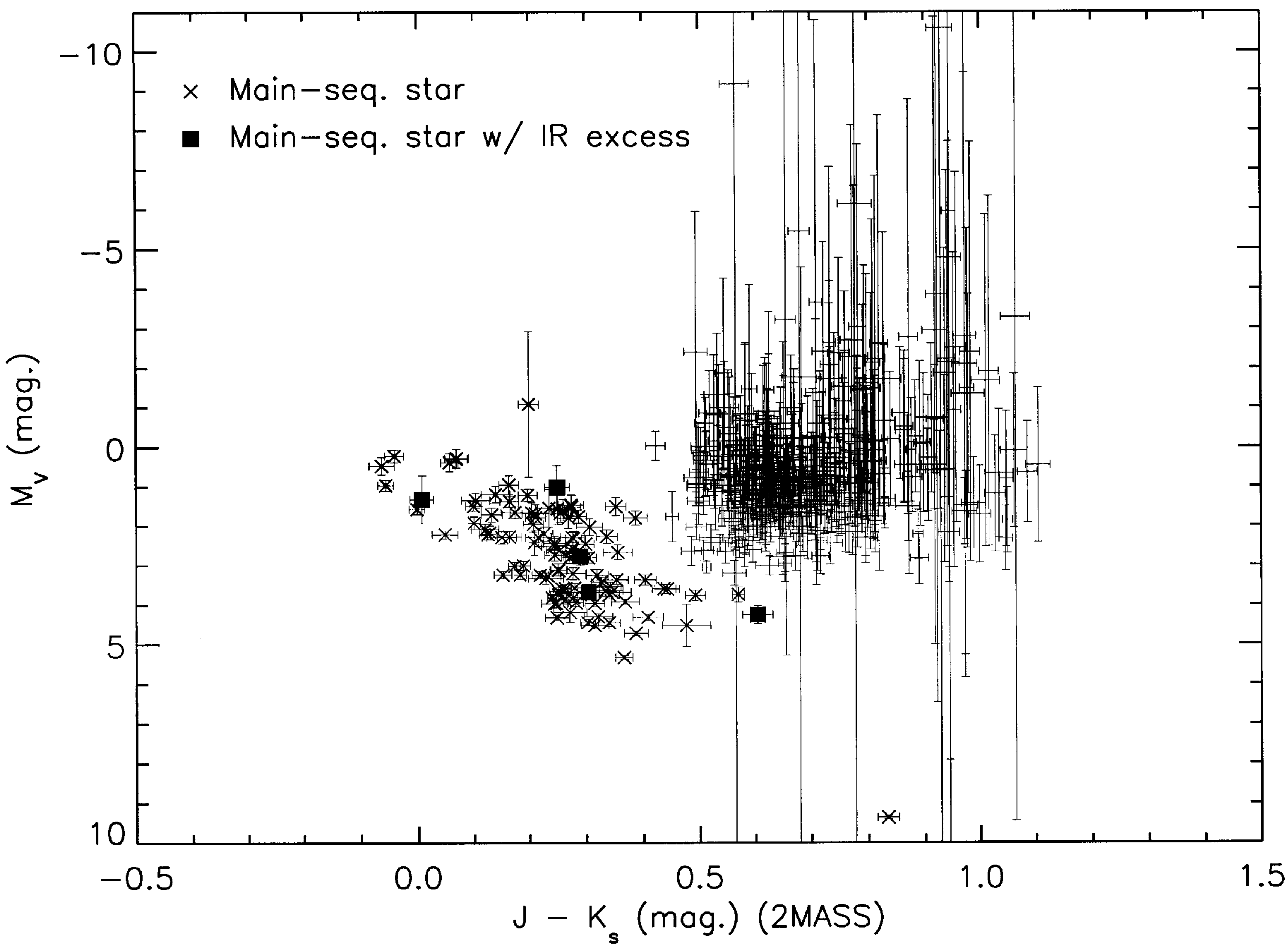
× Main-seq. star
■ Main-seq. star w/ IR excess
−10
−5
0
5
10
−0.5
0.0
0.5
1.0
1.5
M_V (mag.)
$J - K_s$ (mag.) (2MASS)

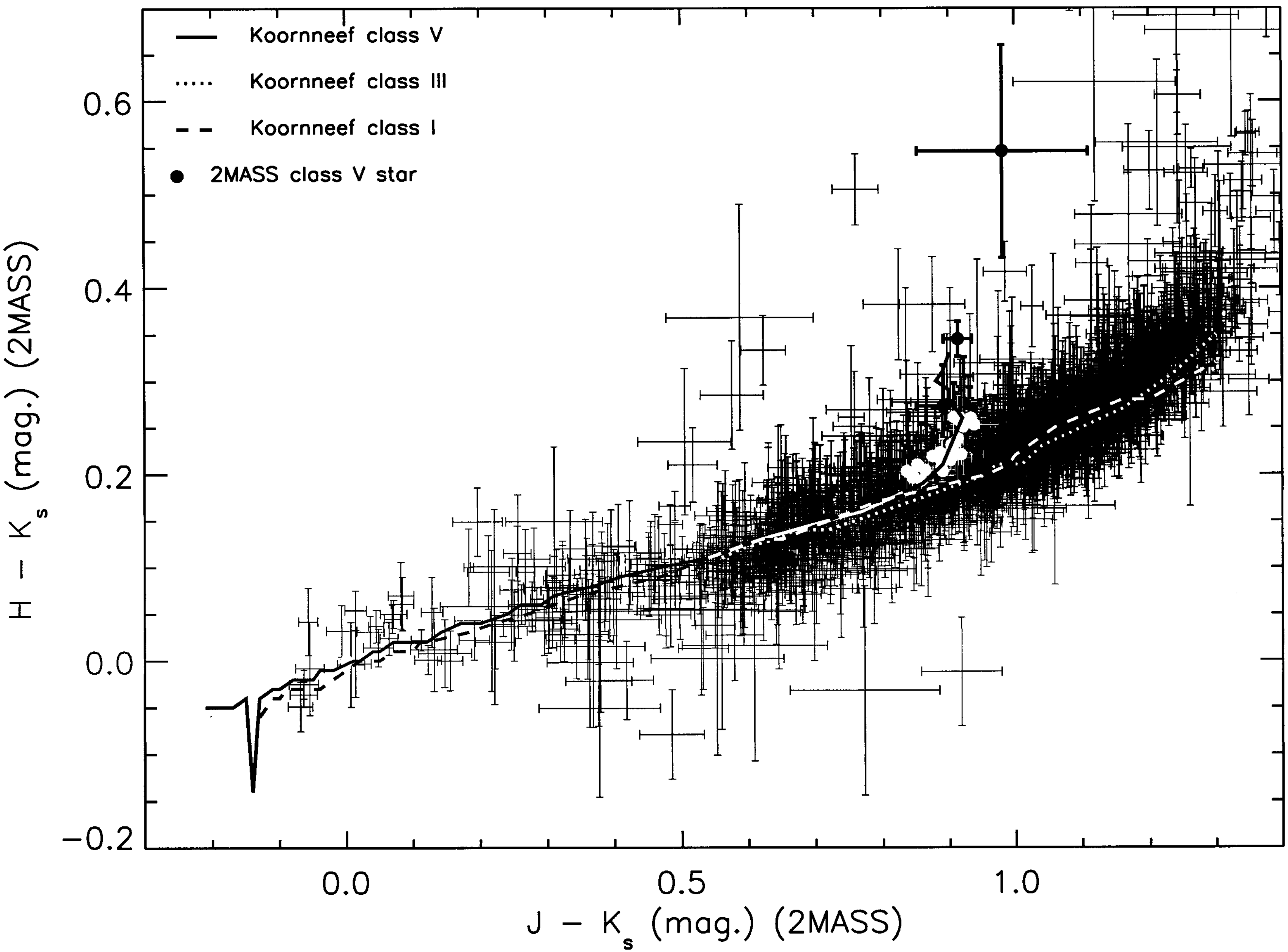

Koornneef class V
Koornneef class III
Koornneef class I
2MASS class V star
0.6
0.4
0.2
0.0
−0.2
H − K s (mag.) (2MASS)
0.0
0.5
1.0
J − K s (mag.) (2MASS)

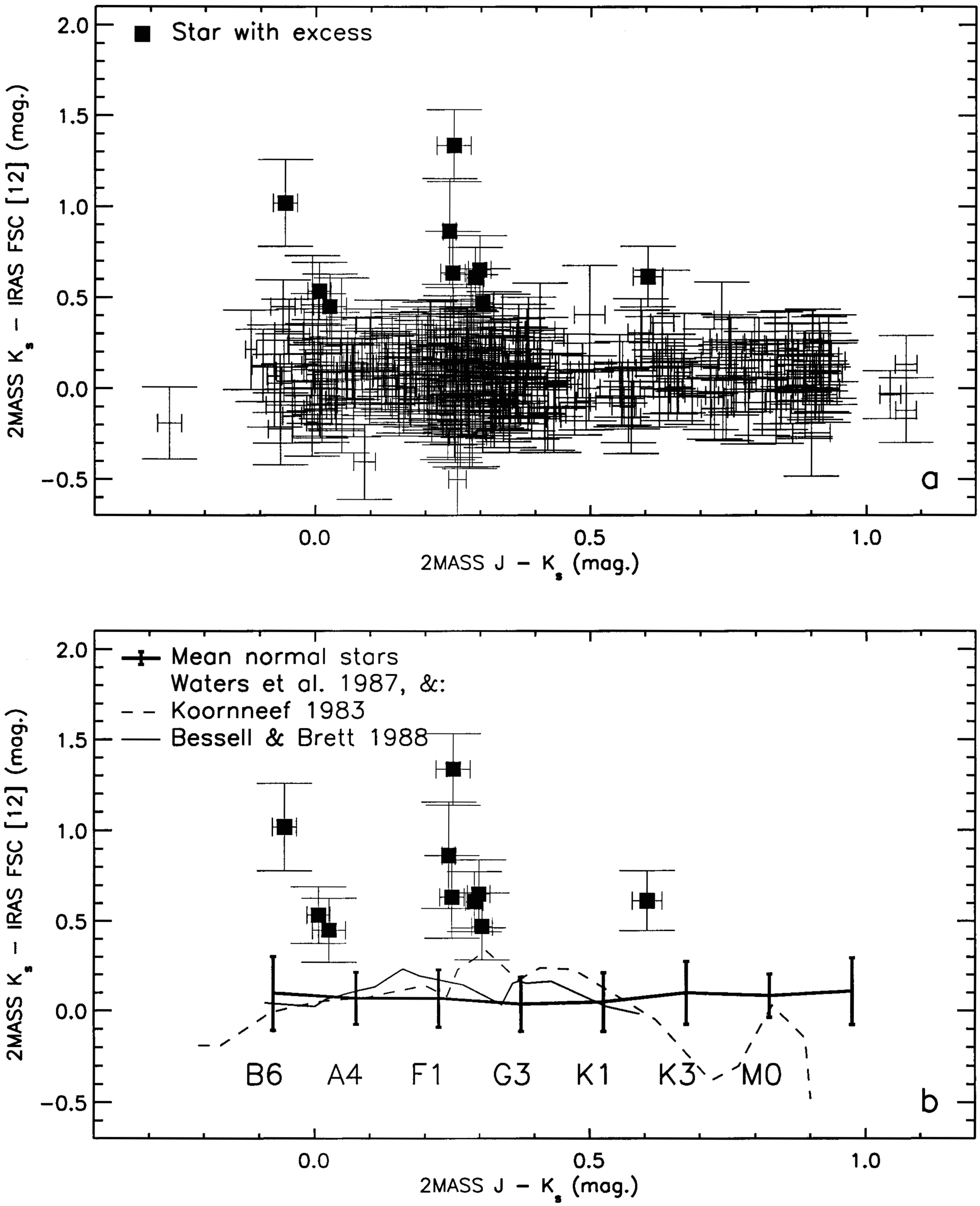
Star with excess
2MASS K$_s$ − IRAS FSC [12] (mag.)
2MASS J − K$_s$ (mag.)
a
Mean normal stars
Waters et al. 1987, &:
Koornneef 1983
Bessell & Brett 1988
B6
A4
F1
G3
K1
K3
M0
b

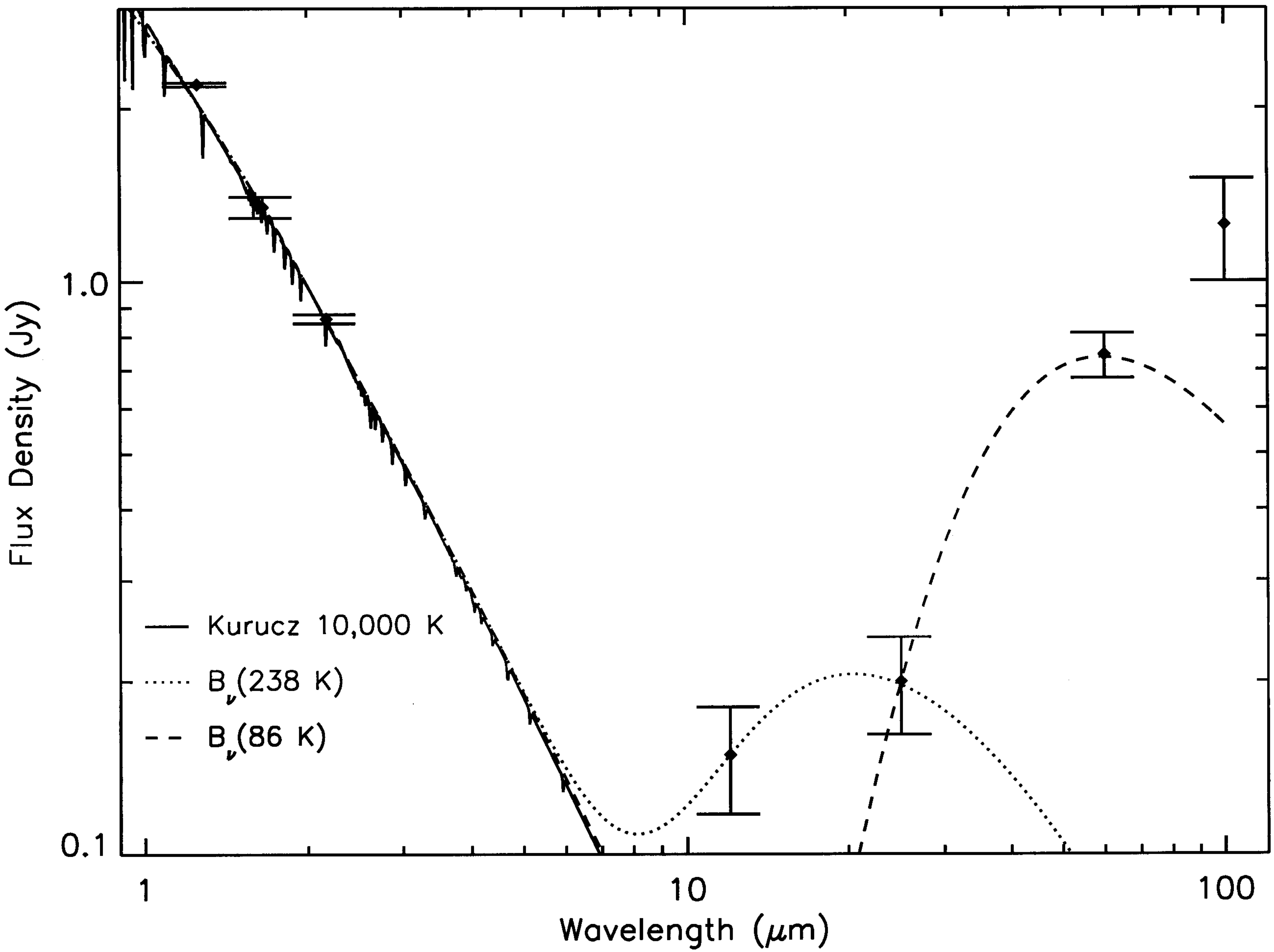

Kurucz 10,000 K
B_ν(238 K)
B_ν(86 K)
Flux Density (Jy)
1.0
0.1
1
10
100
Wavelength (μm)